Effect of squeezing on the degenerate parametric oscillator

Javed Anwar and M. Suhail Zubairy
Department of Electronics, Quaid-i-Azam University, Islamabad, Pakistan
(Received 27 June 1991)

The effect of squeezing on the degenerate parametric oscillator is studied. It is shown that when the ordinary-vacuum reservoir is replaced by a squeezed-vacuum reservoir, the maximum 50% limit of the second-order squeezing inside the cavity can be crossed. It is also shown that the mean number of photons increases considerably. An exact steady-state solution for the Fokker-Planck equation for the field mode is also presented. The photon distribution for the intracavity field and the higher-order variances have been obtained by using the solution of this equation.

PACS number(s): 42.50.Dv, 42.65.Ky, 42.60.Da

I. INTRODUCTION

The subject of squeezing of an electromagnetic field receives attention because a field in a squeezed quantum state has fluctuations reduced below the quantum limit in one quadrature component at the expense of enhanced fluctuations in the canonically conjugate quadrature [1]. A quadrature of the electromagnetic field with reduced fluctuations has attractive applications in optical communication, photondetection techniques, gravitational-wave detection, noise-free amplification, etc.

Because of the inherent two-photon nature of interaction, the parametric processes have been studied as a source of squeezed radiation. Takahashi [2] first pointed out that a degenerate parametric amplifier (DPA) decreases quantum fluctuations in one quadrature phase of the signal at the expense of increased fluctuations in the conjugate quadrature. With the introduction of squeezed states, several authors have considered this system [3–5]. In a DPA, 100% squeezing of a single-mode field can be achieved. Further, the output field is in an ideal squeezed state.

The $\chi^{(2)}$ nonlinearity is typically quite weak, and so in experiments the nonlinear crystal is placed inside an optical cavity [6] to increase the interaction time. In this oscillator configuration, the field experiences losses through one or two partially reflecting end mirrors. Milburn and Walls [7] have shown that the best squeezing attainable in the internal modes of the cavity is a reduction in fluctuations by a factor of 2 at the oscillation threshold, which was also confirmed by Lugiato and Strini [8]. It has been shown by Yurke [9], however, that the output field from a parametric oscillator is perfectly squeezed.

A limit of 50% squeezing of the intracavity field in a degenerate parametric oscillator (DPO) arises from the leakage through the out-coupling mirror and the inevitable amplification of the vacuum fluctuations in the cavity. Since a vacuum field has no definite phase, squeezing of the cavity field is degraded. If, on the other hand, one replaces the ordinary vacuum "environment," one expects that the fluctuations entering the cavity would be biased in the two quadratures, and for a particular phase choice squeezing can be enhanced. Such a scheme has also been proposed by Gea-Banacloche [10] in the context of a single-mode laser. In this paper we show that by using this arrangement, the limit of 50% squeezing of the intracavity field can be surpassed. We also show that under certain limits on the parametric gain-to-loss ratio and on the squeeze parameter, the photon statistics of the cavity field are identical to the ideal two-photon squeezed vacuum.

The organization of the paper is as follows. In Sec. II we have calculated the equations of motion for the first- and second-order moments of the field from the density-matrix equation of motion when the field modes are coupled to the "squeezed vacuum" instead of the ordinary vacuum. The time-dependent solutions of these moments are then used to evaluate the time-dependent squeezing. In Sec. III an exact steady-state solution of the Fokker-Planck equation in the Q representation has been obtained. In Sec. IV the photon distribution function for the cavity field is obtained and its dependence on the squeeze parameter and parametric gain-to-loss ratio is discussed. In Sec. V the higher-order variances have been calculated using the steady-state solution of the Fokker-Planck equation. Finally Sec. VI contains a discussion of our results and conclusions.

II. DEGENERATE PARAMETRIC OSCILLATOR

In a degenerate parametric oscillator a strong pump field of frequency 2ω interacts with a nonlinear medium inside a cavity and gives rise to a field of frequency ω. This process is described at exact resonance and in the rotating-wave approximation by the Hamiltonian (in the interaction picture)

$$H=i\kappa[a^2\exp(i\phi)-a^{\dagger 2}\exp(-i\phi)] . \quad (1)$$

where a and $a^\dagger$ are the annihilation and creation operators for the signal field, κ is the coupling constant, and ϕ is the phase of the pump field. In the following we choose $\phi=0$ for simplicity. We consider one end mirror of the optical cavity to be partially transmitting, through which, instead of the ordinary vacuum, a multimode squeezed vacuum centered around the frequency ω couples to the field inside the cavity. The equation of motion for the density matrix is given by [11]

$$\dot{\rho}=\kappa[H,\rho]-\frac{\gamma}{2}\cosh^2(r)(a^\dagger a\rho-2a\rho a^\dagger+\rho a^\dagger a)-\frac{\gamma}{2}\sinh^2(r)(aa^\dagger\rho-2a^\dagger\rho a+\rho aa^\dagger)$$
$$+\frac{\gamma}{2}e^{-2i\theta}\sinh(r)\cosh(r)(aa\rho-2a\rho a+\rho aa)+\frac{\gamma}{2}e^{2i\theta}\sinh(r)\cosh(r)(a^\dagger a^\dagger\rho-2a^\dagger\rho a^\dagger+\rho a^\dagger a^\dagger)\ , \tag{2}$$

where γ is the cavity relaxation rate, r is the squeeze parameter, and θ is the reference phase for the squeezed field. From Eq. (2) we calculate the equations of motion for the first- and the second-order moments of the field as

$$\langle a\rangle^{\cdot}=-2\kappa\langle a^\dagger\rangle-\frac{\gamma}{2}\langle a\rangle\ , \tag{3}$$

$$\langle a^2\rangle^{\cdot}=-4\kappa\langle a^\dagger a\rangle-\gamma\langle a^2\rangle+\gamma e^{2i\theta}\sinh(r)\cosh(r)-2\kappa\ . \tag{4a}$$

$$\langle a^\dagger a\rangle^{\cdot}=-2\kappa\langle a^{\dagger 2}\rangle-2\kappa\langle a^2\rangle-\gamma\langle a^\dagger a\rangle+\gamma\sinh^2(r)\ . \tag{4b}$$

The time-dependent *solutions* of these equations are

$$\langle a\rangle_t=e^{-\gamma t/2}[\langle a\rangle_0\cosh(2\kappa t)-\langle a^\dagger\rangle_0\sinh(2\kappa t)]\ . \tag{5}$$

$$[\langle a^2+a^{\dagger 2}\rangle]_t=\{e^{-\gamma t}[-2\langle a^\dagger a\rangle_0\sinh(4\kappa t)+(\langle a^2\rangle_0+\langle a^{\dagger 2}\rangle_0)\cosh(4\kappa t)$$
$$-\gamma^2\sinh(2r)\cosh(4\kappa t)\cos(2\theta)-4\gamma\kappa\sinh(2r)\sinh(4\kappa t)\cos(2\theta)+2\gamma^2\sinh^2(r)\sinh(4\kappa t)$$
$$+8\gamma\kappa\sinh^2(r)\cosh(4\kappa t)+4\gamma\kappa\cosh(4\kappa t)+16\kappa^2\sinh(4\kappa t)]$$
$$+\gamma^2\sinh(2r)\cos(2\theta)-8\gamma\kappa\sinh^2(r)-4\gamma\kappa\}/(\gamma^2-16\kappa^2)\ . \tag{6a}$$

$$\langle a^\dagger a\rangle_t=\{e^{-\gamma t}[\langle a^\dagger a\rangle_0\cosh(4\kappa t)-\tfrac{1}{2}(\langle a^2\rangle_0+\langle a^{\dagger 2}\rangle_0)\sinh(4\kappa t)-\gamma^2\sinh^2(r)\cosh(4\kappa t)$$
$$-4\gamma\kappa\sinh^2(r)\sinh(4\kappa t)+\frac{\gamma^2}{2}\sinh(2r)\sinh(4\kappa t)\cos2\theta$$
$$+2\gamma\kappa\sinh(2r)\cosh(4\kappa t)\cos(2\theta)-2\gamma\kappa\sinh(4\kappa t)-8\kappa^2\cosh(4\kappa t)]$$
$$+\gamma^2\sinh^2(r)-2\gamma\kappa\sinh(2r)\cos(2\theta)+8\kappa^2\}/(\gamma^2-16\kappa^2)\ . \tag{6b}$$

where $\langle a\rangle_0$ and $\langle a^\dagger a\rangle_0$, etc. represent the initial moments of the field.

Defining the filed quadratures as

$$a_1=\tfrac{1}{2}(a+a^\dagger)\ , \tag{7a}$$

$$a_2=\frac{1}{2i}(a-a^\dagger)\ , \tag{7b}$$

the variances of these Hermitian amplitudes are

$$(\Delta a_1^2)_t=\tfrac{1}{4}(\langle a^2\rangle_t+\langle a^{\dagger 2}\rangle_t+2\langle a^\dagger a\rangle_t-\langle a+a^\dagger\rangle_t^2)+\tfrac{1}{4}\ , \tag{8}$$

$$(\Delta a_2^2)_t=\tfrac{1}{4}(\langle a^\dagger\rangle_t+\langle a^{\dagger 2}\rangle_t-2\langle a^\dagger a\rangle_t-\langle a+a^\dagger\rangle_t^2)+\tfrac{1}{4}\ . \tag{9}$$

On substituting the values of $\langle a\rangle_t^2$, $\langle a^\dagger\rangle_t^2$, $\langle a^2\rangle_t$, $\langle a^{\dagger 2}\rangle_t$, and $\langle a^\dagger a\rangle_t$ in the above equation, we obtain the following expressions for the time-dependent-quadrature variances:

$$(\Delta a_1)_t^2=(\Delta a_1)_0^2e^{-\gamma(1+2s)t}$$
$$+\tfrac{1}{4}(1-e^{-\gamma(1+2s)t})$$
$$\times\left[\frac{\cosh(2r)+\sinh(2r)\cos(2\theta)}{(1+2s)}\right]\ , \tag{10}$$

$$(\Delta a_2)_t^2=(\Delta a_2)_0^2e^{-\gamma(1-2s)t}$$
$$+\tfrac{1}{4}(1-e^{-\gamma(1-2s)t}$$
$$\times\left[\frac{\cosh(2r)-\sinh(2r)\cos(2\theta)}{(1-2s)}\right]\ , \tag{11}$$

where $s=2\kappa/\gamma$ is the ratio of the parametric gain to the parametric loss and $(\Delta a_1)_0^2$ and $(\Delta a_2)_0^2$ represent the initial variances of the two quadratures. An analysis of Eqs. (10) and (11) can be made by taking the "squeeze phase" choice $\theta=\pi/2$. The uncertainties in the output quadrature phases then have the simple form

$$(\Delta a_1)_t^2=G_1(\Delta a_1)_0^2+\Delta F_1^2(1-G_1)\ , \tag{12a}$$

$$(\Delta a_2)_t^2=G_2(\Delta a_2)_0^2+\Delta F_2^2(1-G_2)\ , \tag{12b}$$

where

$$G_1=e^{-\gamma(1+2s)t}\ , \tag{13a}$$

$$G_2=e^{-\gamma(1-2s)t} \tag{13b}$$

are the gain factors for the two quadratures and

$$(\Delta F_1)^2=\tfrac{1}{4}\left[\frac{e^{-2r}}{1+2s}\right]\ , \tag{14a}$$

$$(\Delta F_2)^2=\frac{1}{4}\left[\frac{e^{+2r}}{1-2s}\right] \tag{14b}$$

represent the added noise in the two quadratures, respectively. The plot in Fig. 1 shows $(\Delta a_1)^2$ versus γt for different values of the squeeze parameter r. As $t\to\infty$, G_1 and $G_2\to 0$, and at the pump threshold, i.e., $s=0.5$,

$$(\Delta a_1)^2_{st}=\frac{1}{8}e^{-2r}, \tag{15a}$$

$$(\Delta a_2)^2_{st}\to\infty . \tag{15b}$$

These equations, for $r=0$, obviously confirm the previous findings for the DPO, i.e., the maximum reduction in fluctuations that may be achieved in an ideal DPO is a factor of 2 for a device operated in the region of threshold. For $r>0$, i.e., when the external field is in a squeezed-vacuum state, squeezing is larger than 50%. It is interesting to note that the factor e^{-2r} appearing in Eq. (15a) is the same factor by which the fluctuations in the outside vacuum are squeezed. This squeezing is further increased by a factor of $\frac{1}{2}$ coming from the parametric process. That is, the total squeezing is simply the product of the factor by which the outside vacuum is squeezed and the factor $\frac{1}{2}$ by which an ordinary DPO squeezes the field in the steady state. In the steady state, the mean number of photons can be obtained from Eq. (6b) as

$$\langle a^\dagger a\rangle_{st}=[\sinh^2(r)-s\sinh(2r)\cos(2\theta)+2s^2]/[1-4s^2] . \tag{16}$$

In Eq. (16) the first term represents the mean number of photons in a squeezed vacuum and the third term gives the mean number of photons in the DPO. The phase-dependent contribution (second term) arises due to coupling of the intracavity field due to the squeezed reservoir. Equation (16) therefore tells us that the mean photon number is not just the sum of the number of photons in the DPO and the number of photons entering the cavity from the squeezed reservoir. This point is further elucidated in Fig. 2 in which the mean photon number is plotted against the squeezed parameter r. Curve (a) shows $\bar{n}$ from Eq. (16) while curve (b) shows $\bar{n}$ in the reservoir. The baseline (c) indicates the mean number of photons in the DPO with an ordinary vacuum reservoir. In this setup, then, considerable amplification is achieved.

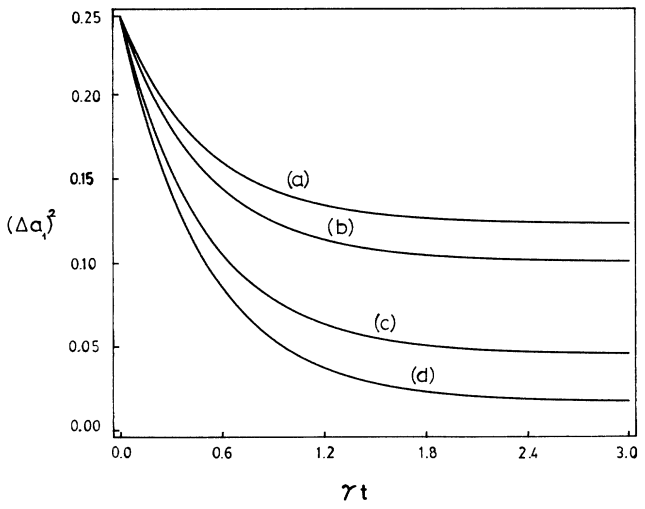

FIG. 1. $(\Delta a_1)^2$ vs γt for $s=0.49$, $\theta=\pi/2$ and (a) $r=0$, (b) $r=0.1$, (c) $r=0.5$, (d) $r=1$.

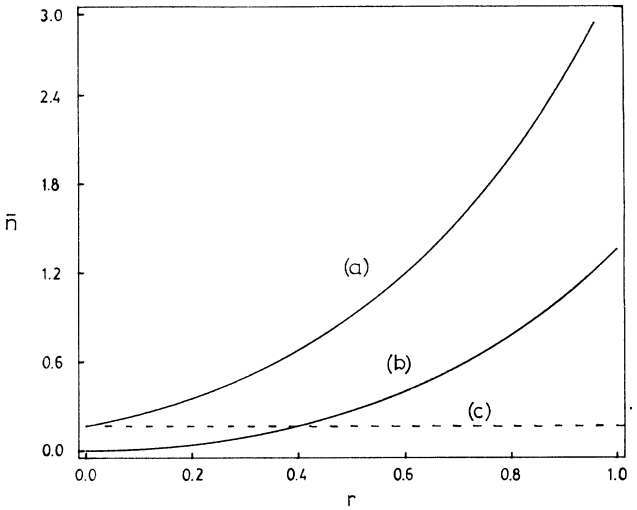

FIG. 2. $\bar{n}$ vs r for the DPO, $s=0.25$. (a) Coupled to a squeezed-vacuum reservoir. (b) $\bar{n}$ in the reservoir. The baseline (c) shows $\bar{n}$ in the absence of a squeezed reservoir.

III. FOKKER-PLANCK EQUATION AND ITS EXACT STEADY-STATE SOLUTION USING THE Q REPRESENTATION

In this section we derive the Fokker-Planck equation using the Q representation instead of the commonly used P representation. This disadvantage of using the P representation is that it becomes non-positive-definite for the nonclassical states like the number state or the squeezed state. The Q representation can be used to evaluate the expectation values of the antinormally ordered operators which are essentail for the determination of quadrature variances of the field.

The representation for the antinormal distribution function in terms of the density operator is

$$Q(\alpha,\alpha^*)=\frac{1}{\pi}\langle\alpha|\rho|\alpha\rangle , \tag{17}$$

where $|\alpha\rangle$ is a coherent state.

The expectation value of any antinormally ordered function $\mathcal{O}(a,a^\dagger)$ may be determined from $Q(\alpha,\alpha^*)$ from the relation

$$\langle\mathcal{O}(a,a^\dagger)\rangle=\int\mathcal{O}(\alpha,\alpha^*)Q(\alpha,\alpha^*)d^2\alpha , \tag{18}$$

We take expectation values of Eq. (2) with respect to the coherent state and obtain the equation of motion

$$\frac{\partial Q}{\partial t}=\left[\kappa\left[\frac{\partial^2}{\partial\alpha^2}+2\alpha^*\frac{\partial}{\partial\alpha}\right]+\frac{\gamma}{2}\frac{\partial}{\partial\alpha}\alpha+\frac{\gamma}{2}\cosh^2(r)\frac{\partial^2}{\partial\alpha\partial\alpha^*}+\frac{\gamma}{2}e^{2i\theta}\sinh(r)\cosh(r)\frac{\partial^2}{\partial\alpha^2}\right]Q+\text{c.c.} \tag{19}$$

Here α can be expressed in terms of real and imaginary parts,

$$\alpha=x_1+ix_2\ , \tag{20a}$$

$$\alpha^*=x_1-ix_2\ . \tag{20b}$$

It follows from Eqs. (20a) and (20b) that

$$\frac{\partial}{\partial\alpha}=\tfrac{1}{2}\left[\frac{\partial}{\partial x_1}-i\frac{\partial}{\partial x_2}\right] \tag{21a}$$

and

$$\frac{\partial}{\partial\alpha^*}=\tfrac{1}{2}\left[\frac{\partial}{\partial x_1}+i\frac{\partial}{\partial x_2}\right]\ . \tag{21b}$$

We denote the function $Q(\alpha,\alpha^*)$ by $F(x_1,x_2)$, when expressed in terms of real variables x_1,x_2. It follows from Eq. (19) that $F(x_1,x_2)$ satisfies the following Fokker-Planck equation [12]:

$$\frac{\partial F}{\partial t}=\sum_{i=1}^{2}\frac{\partial}{\partial x_i}\left[A_i x_i+\sum_{j=1}^{2}B_{ij}\frac{\partial}{\partial x_j}\right]F\ , \tag{22}$$

where

$$A_1=\frac{\gamma}{2}(1+2s)\ , \tag{23a}$$

$$A_2=\frac{\gamma}{2}(1-2s)\ , \tag{23b}$$

$$B_{11}=\frac{\gamma}{4}[\cosh^2(r)+\sinh(r)\cosh(r)\cos(2\theta)+s]\ , \tag{23c}$$

$$B_{22}=\frac{\gamma}{4}[\cosh^2(r)-\sinh(r)\cosh(r)\cos(\theta)-s]\ , \tag{23d}$$

$$B_{12}=B_{21}=\frac{\gamma}{2}\cosh(r)\sinh(r)\sin(2\theta)\ . \tag{23e}$$

In the steady state, $\partial F/\partial t=0$, and Eq. (22) reduces to the following pair of differential equations:

$$\frac{\partial F}{\partial x_1}=-\left[\frac{A_1B_{22}x_1-A_2B_{12}x_2}{A_{12}B_{21}-B_{22}B_{11}}\right]F\ , \tag{24a}$$

$$\frac{\partial F}{\partial x_2}=-\left[\frac{A_2B_{11}x_2-A_1B_{21}x_1}{B_{21}B_{12}-B_{11}B_{22}}\right]F\ . \tag{24b}$$

On substituting the values of A_i and B_{ij} from Eqs. (23a)–(23e), we get

$$\frac{\partial F}{\partial x_1}=2\left[\frac{(1+2s)(C_1-C_2-s)x_1-(1-2s)C_3x_2}{C_3^2-(C_1+C_2+s)(C_1-C_2-s)}\right]F\ , \tag{25a}$$

$$\frac{\partial F}{\partial x_2}=2\left[\frac{(1-2s)(C_1+C_2+s)x_1-(1+2s)C_3x_2}{C_3^2-(C_1+C_2+s)(C_1-C_2-s)}\right]F\ , \tag{25b}$$

where

$$C_1=\cosh^2(r)\ , \tag{26a}$$

$$C_2=\sinh(r)\cosh(r)\cos(2\theta)\ , \tag{26b}$$

$$C_3=\sinh(r)\cosh(r)\sin(2\theta)\ . \tag{26c}$$

The solution of Eqs. (25a) and (25b) is given by

$$F(x_1,x_2)=\frac{1}{N}e^{-\beta_1x_1^2-\beta_2x_2^2+(\beta_3+\beta_4)x_1x_2}\ , \tag{27}$$

where

$$\beta_1=\left[\frac{(1+2s)(C_1-C_2-s)}{(C_1+C_2+s)(C_1-C_2-s)-C_3^2}\right]\ , \tag{28a}$$

$$\beta_2=\left[\frac{(1-2s)(C_1+C_2+s)}{(C_1+C_2+s)(C_1-C_2-s)-C_3^2}\right]\ , \tag{28b}$$

$$\underset{(4)}{\beta_3}=\left[\frac{(1-2s)\underset{(+)}{C_3}}{(C_1+C_2+s)(C_1-C_2-s)-C_3^2}\right]\ , \tag{28c}$$

subject to the condition that

$$\beta_3=\beta_4\ . \tag{29}$$

Condition (29) is satisfied when (i) $s=0$ or (ii) $\theta=0$, $\pi/2$. In the following, therefore, we restrict our analysis to the phase choice $\theta=0$ or $\pi/2$. Under this condition, $C_3=0$ and the solution for $Q(\alpha,\alpha^*)$ is given by

$$Q(\alpha,\alpha^*)=\frac{(\beta_1\beta_2)^{1/2}}{\pi}e^{-(\beta_1/4)(\alpha+\alpha^*)^2+(\beta_2/4)(\alpha-\alpha^*)^2}\ . \tag{30}$$

Here we have determined N from the normalization condition, i.e.,

$$\frac{1}{N}\int_{-\infty}^{+\infty}e^{-\beta_1x_1^2-\beta_2x_2^2}dx_1dx_2=1\ . \tag{31}$$

We now have an exact steady-state solution of the Fokker-Planck equation for the field mode. In the absence of nonlinear coupling, i.e., for $\kappa=0$, Eq. (30) reduces to the complex Q representation for an ideal squeezed-vacuum state,

$$Q(\alpha,\alpha^*,r)=\frac{\text{sech}(r)}{\pi}e^{[-|\alpha|^2-(1/2)(\alpha^2+\alpha^{*2})\tanh(r)]}\ . \tag{32}$$

Apparently, the Q representation for a DPO coupled to a squeezed vacuum through cavity relaxation is quite similar in form to Eq. (32) for an ideal squeezed vacuum. It should be noted, however, that the cavity field is not in an ideal squeezed state. This result agrees with an earlier result obtained by Collet and Gardiner [13] in which they predicted a perfect squeezed vacuum by shining the light from a DPO into an empty cavity. In the following sections we will use this solution to evaluate the photon statistics and higher-order squeezing.

IV. PROBABILITY DISTRIBUTION FUNCTION

The photon distribution function $p(n)$ for the field can be determined by using the relation

$$p(n)=\langle n|\rho_F|n\rangle \ . \tag{33}$$

In terms of the Q representation, this distribution function can be written

$$p(n)=\frac{\pi}{n!N}\left[\frac{\partial^{2n}}{\partial\alpha^n\partial\alpha^{*n}}e^{[-(\beta_1/4)(\alpha+\alpha^*)^2+(\beta_2/4)(\alpha-\alpha^*)^2+|\alpha|^2]}\right]_{\alpha=\alpha^*=0} . \tag{35}$$

After carrying out the nth-order differentiation of the above function and applying the condition $\alpha=\alpha^*=0$, we get the photon probability distribution function

$$p(n)=\frac{(\beta_1\beta_2)^{1/2}}{2^n n!}(\beta_1-1)^n \times\left[\sum_{k=0}^{n}\binom{n}{k}\frac{1}{2^n}H_{2(n-k)}(0)H_{2k}(0)\left[\frac{1-\beta_2}{1-\beta_1}\right]^k\right] . \tag{36}$$

This is the general result for the photon distribution function for a DPO coupled to a squeezed-vacuum field through an end mirror. In the following we discuss two limiting cases for this distribution.

(i) For $r=0$, Eq. (36) reduces to

$$p(n)=\left[\frac{1-4s^2}{1-s^2}\right]\left[\frac{s}{2(1+s)}\right]^n\frac{1}{n!} \times\sum_{k=0}^{n}\binom{n}{k}\frac{1}{2^n}H_{2(n-k)}(0) \times H_{2k}(0)(-1)^k\left[\frac{1+s}{1-s}\right]^k . \tag{37}$$

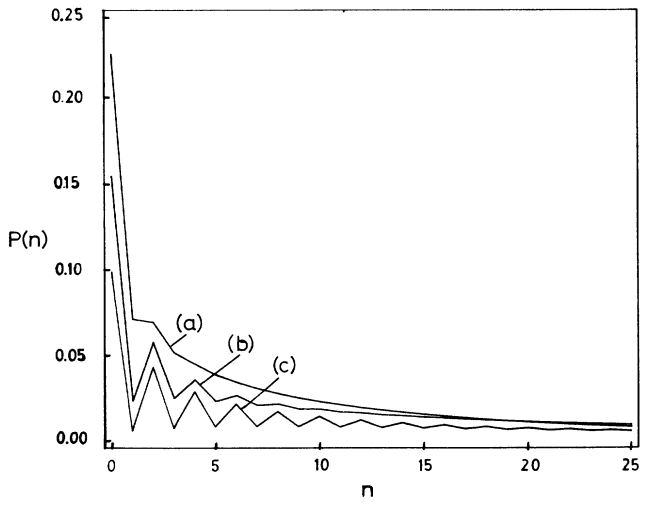

FIG. 3. $p(n)$ vs n for $s=0.49$, $\theta=\pi/2$ and (a) $r=0$, (b) $r=0.5$, (c) $r=1$.

$$p(n)=\frac{\pi}{n!}\left[\frac{\partial^{2n}}{\partial\alpha^n\partial\alpha^{*n}}[Q(\alpha,\alpha^*)e^{|\alpha|^2}]\right]_{\alpha=\alpha^*=0} , \tag{34}$$

which can be determined from the knowledge of $Q(\alpha,\alpha^*)$ and from the properties of coherent states [14]. On substituting the value of $Q(\alpha,\alpha^*)$ from Eq. (30) into Eq. (34), we get the following form for $p(n)$:

This gives the photon distribution for a DPO, which, to our knowledge, has not been reported earlier. The effect of cavity damping is now apparent from Eq. (37), wherein we see that there is a finite probability for an odd number of photons.

(ii) In the limit when

$$r\gg-\tfrac{1}{2}\ln(1-2s) , \tag{38}$$

all odd ordered terms in Eq. (36) are zero and the photon distribution function reduces to that for a squeezed vacuum:

$$p(n)=\begin{cases}\dfrac{(-1)^n[1/2\tanh(r)]^{2n}}{n!\cosh(r)}H_{2n}(0) & \text{for even } n\\ 0 \quad \text{for odd } n \ .\end{cases} \tag{39}$$

In this limit, therefore, the photon distribution function of the field is identical to that for an ideal two-photon squeezed state. In Fig. 3, $p(n)$ is plotted versus n for different values of the squeeze parameter r. Clearly, as condition (38) is approached, oscillations begin to appear in $p(n)$ and the distribution function looks similar to that for an ideal two-photon squeezed state [15].

V. HIGHER-ORDER STEADY-STATE SQUEEZING

In this section we obtain steady-state expressions for the higher-order variances—in particular, fourth and sixth order—of the field. As defined by Hong and Mandel [16], a field is squeezed to Nth order if its Nth-order, normally ordered variance $\langle:(\Delta a_i)^N:\rangle$ is less than the coherent-state value.

A. Fourth-order squeezing

The state of the field is squeezed to the fourth order if it satisfies

$$q_4\equiv[\langle:(\Delta a_i)^4:\rangle+\tfrac{6}{4}\langle:(\Delta a_i)^2:\rangle]<0 , \tag{40}$$

where

$$\langle:(\Delta a_1)^4:\rangle=\tfrac{1}{16}[\langle a^4\rangle+\langle a^{\dagger 4}\rangle+6\langle a^{\dagger 2}a^2\rangle +4\langle a^\dagger a^3\rangle+4\langle a^{\dagger 3}a\rangle] . \tag{41}$$

The steady-state expectation values of the operators in Eq. (41) can be calculated from the expression of $Q(\alpha,\alpha^*)$. Thus, by using Eq. (17), we get

$$\langle :(\Delta a_1)^4: \rangle = \tfrac{3}{16}\left[\frac{C_1+C_2-s-1}{(1+2s)}\right]^2 . \tag{42}$$

B. Sixth-order squeezing

The state of the field is squeezed to the sixth order if it satisfies

$$q_6 \equiv [\langle :(\Delta a_i)^6: \rangle + \tfrac{15}{4}\langle :(\Delta a_i)^4: \rangle + \tfrac{45}{16}\langle :(\Delta a_i)^2: \rangle] < 0 , \tag{43}$$

where in a similar manner as before we can calculate the expectation value of the sixth-order moment, which is

$$\langle :(\Delta a_1)^6: \rangle = [8(C_1^3+C_2^3)+24C_1C_2(C_1+C_2)-24s^2(C_1+C_2)-24s(C_1+C_2) - 12(C_1^2+C_2^2)-24C_1C_2-24s^2(s+1)-6s-1]/16(1+2s)^3 . \tag{44}$$

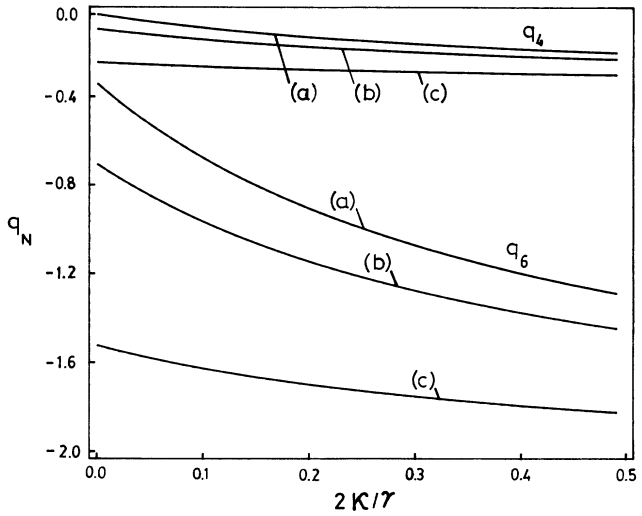

FIG. 4. q_N vs s for $s=0.49$, $\theta=\pi/2$ and (a) $r=0$, (b) $r=0.1$, (c) $r=0.5$.

In Fig. 4 we have plotted the higher-order variances versus the parametric gain-to-loss ratio s for the phase choice $\theta=\pi/2$ and for different values of the squeeze parameter r. Since higher-order squeezing depends upon the value of the squeeze parameter r, which is also evident from these figures, showing that fractional increase in the value of r increases the initial fourth- and higher-order squeezing. The DPO enhances the initial higher-order squeezing as we increase the value of the parametric gain relative to the loss. We get maximum steady-state squeezing near the pump threshold.

VI. CONCLUSION

We have analyzed the effect of a squeezed-vacuum reservoir on a degenerate parametric oscillator. It is shown that the maximum 50% limit of second-order steady-state squeezing inside a cavity can be surpassed when operating in the region of the oscillation threshold. It is shown that the total squeezing inside the cavity in the steady state and at the threshold is simply the product of the factor $\frac{1}{4}\exp(-2r)$ by which the outside vacuum is squeezed and a factor of $\frac{1}{2}$ arising from the ordinary degenerate parametric oscillator [see Eq. (15a)]. Further, the cavity field is amplified and the mean photon number increases considerably. We have also calculated the photon distribution function $p(n)$ and have studied its dependence on the squeezing parameter r and on the parametric gain-to-loss ratio s. We have also studied higher-order squeezing in the DPO and have shown that higher-order squeezing depends upon the squeeze parameter r.

ACKNOWLEDGMENTS

We wish to thank Dr. Nadeem A. Ansari and Dr. Khalid Zaheer for useful discussions. This research was supported by grants from the Pakistan Science Foundation and the Pakistan Atomic Energy Commission.

[1] K. Zaheer and M. S. Zubairy, in *Advances in Atomic, and Molecular and Optical Physics,* edited by D. R. Bates and B. Bederson (Academic, New York, 1990), Vol. 28, p. 143.
[2] H. Takahashi, Adv. Commun. Syst. **1**, 227 (1965).
[3] D. Stoler, Phys. Rev. Lett. **33**, 1397 (1974).
[4] H. P. Yuen, Phys. Rev. A **13**, 2226 (1976).
[5] L. Mista, V. Perinova, J. Perina, and Z. Braunerova, Acta. Phys. Pol. A **51**, 739 (1977).
[6] For details of the experiment, see L. A. Wu, M. Xiao, and H. J. Kimble, J. Opt. Soc. Am. B **4**, 1465 (1987).
[7] G. Milburn and D. F. Walls, Opt. Commun. **39**, 401 (1981).
[8] L. A. Lugiato and G. Strini, Opt. Commun. **41**, 67 (1982).
[9] B. Yurke, Phys. Rev. A **29**, 408 (1984).
[10] J. Gea-Banacloche, Phys. Rev. Lett. **59**, 523 (1987).
[11] J. Gea-Banacloche, M. O. Scully, and M. S. Zubairy, Phys. Scr. **T21**, 81 (1988).
[12] M. S. Zubairy, Phys. Rev. A **20**, 2464 (1979).
[13] M. J. Collet and C. W. Gardiner, Phys. Rev. A **30**, 1386 (1984).
[14] M. Sargent III, M. O. Scully, and W. E. Lamb, Jr., *Laser Physics* (Addison-Wesley, Reading, MA, 1974).
[15] W. Schleich and J. A. Wheeler, Nature **326**, 574 (1987); J. Opt. Soc. Am. B **4**, 1715 (1987).
[16] C. K. Hong and L. Mandel, Phys. Rev. Lett. **54**, 323 (1985).